Flicker ($1/f$) noise in copper films due to radiation-induced defects

Jonathan Pelz* and John Clarke
Department of Physics, University of California, Berkeley, California 94720
and Materials and Chemical Sciences Division, Lawrence Berkeley Laboratory, Berkeley, California 94720

Wayne E. King†
Division of Materials Science and Technology, Argonne National Laboratory, Argonne, Illinois 60349-4843

(Received 29 April 1988)

Changes were measured in the resistivity and $1/f$ noise in polycrystalline Cu films due to defects induced by 500-keV to 1.1-MeV electron irradiation or 1-MeV Kr^{+}-ion irradiation. Irradiation with 500-keV electrons increased the noise level in films maintained at 90 K by as much as an order of magnitude, while the resistivity increased by at most 10%. When the films were annealed at progressively higher temperatures, both the $1/f$ noise and the resistivity were reduced; however, at lower annealing temperatures, the fractional reduction in the induced noise was substantially more than in the added resistivity. These results suggest that a large fraction of the induced noise is generated by "mobile" added defects that are more readily annealed than the majority of the added defects. The temperature dependence of the noise after irradiation and partial annealing indicated that the induced noise was thermally activated in a manner consistent with the Dutta-Dimon-Horn model. Isolated defects created by 1.1-MeV electron irradiation were found to produce substantially higher noise levels than clustered defects resulting from 1-MeV Kr^{+}ion irradiation. Measurements on a number of films indicate that the induced $1/f$ noise is not sensitive to the type and quantity of interstitial traps. A model which attributes the noise to the motion of defects involving vacancies close to surfaces, grain boundaries, or dislocations is most consistent with the experimental results.

I. INTRODUCTION

Metal films biased with a constant current exhibit low-frequency voltage fluctuations in excess of the equilibrium Johnson noise.[1,2] The spectral density $S_V(f)$ of this excess noise typically scales as $1/f^m$, where f is the frequency and the exponent m has a value close to 1. This "flicker" or "$1/f$" noise is a phenomenon occurring in many physical systems,[2] including semiconductors,[3] ionic solutions,[4] charge-density-wave materials,[5] and electronic devices.[6–13]

In metal films it is generally agreed that the noise is due to intrinsic resistance fluctuations, present even in the absence of a bias current.[14,15] A convenient way to characterize $1/f$ noise is by the frequency exponent m, defined above, and the dimensionless parameter

$$\alpha \equiv N f_0 S_V(f_0)/V^2 = N f_0 S_R(f_0)/R^2 = N f_0 S_\rho(f_0)/\rho^2 \; . \tag{1}$$

Here, V is the voltage across the sample, R and ρ are sample resistance and spatially averaged resistivity, respectively, while $S_R(f)$ and $S_\rho(f)$ are the spectral densities of these quantities, N is the number of atoms in the sample, and f_0 is a reference frequency (typically ~ 1 Hz) chosen within the experimental bandwidth. Equation (1) is equivalent to Hooge's expression[16] except in that he defines N as the number of free charge carriers in the sample. Scofield *et al.*[17] have pointed out that the parameter α tends to be small in materials with a large intrinsic resistivity whether or not that high resistivity is related to the sample noise. They have accordingly proposed an alternate normalization of the noise in terms of a parameter ρ_*^2, defined by

$$\rho_*^2 \equiv N f_0 S_\rho(f_0) = \alpha \rho^2 \; . \tag{2}$$

Early experimental results seemed to indicate that α has nearly the same value in very different physical systems,[16] spurring attempts to formulate a "universal" theory for the noise. However, more recent experimental work has made it abundantly clear that the noise level can vary by many orders of magnitude from system to system,[17] and that the spectra density often differs from a simple power-law form.[6–11,13] Weissman[2] has emphasized that quite diverse mechanisms are responsible for the noise observed in various systems.

Nonetheless, two general properties appear to be common to the $1/f$ noise observed in a variety of physical systems. The $1/f$ spectrum often results from a superposition of Lorentzian spectra, with a broad distribution of characteristic times.[1,6–11,13] Each Lorentzian is thought to be due to a particular microscopic process, which is often thermally activated. Dutta, Dimon, and Horn,[18] expanding on earlier ideas of Du Pre[19] and Van der Ziel,[20] showed that such a superposition of Lorentzians could provide a simple, self-consistent explanation of the observed $1/f$ noise.

It also appears that atomic or defect motion is responsible for the low-frequency noise observed in a variety of systems.[8,10,11,21] The case for defect involvement is particularly strong for metal films. Eberhard and Horn[22] showed that annealing freshly evaporated noble-metal films reduced the $1/f$ noise while it increased crystallite size. Similarly, Fleetwood and Giordano[23] found that annealing substantially lowered the noise and resistivity in AuPd films. Zhigal'skiy *et al.*[24] found that noise levels in metal films depended on internal stresses, while Fleetwood and Giordano[25] showed that externally applied stress could cause large increases in noise. Since defect motion accompanies strain relaxation, these results support the hypothesis that defect motion is a source of $1/f$ noise in metals. Scoffield *et al.*[17] studied $1/f$ noise in a variety of metal films and found that films with the largest residual-resistivity ratio generally had the lowest noise levels (normalized as ρ_*^2). From measurements on Al films doped with Cu and Si, Koch *et al.*[26] found a correlation between "noise" activation energies inferred from the temperature dependence of $S_V(f)$ and those for electromigration failure. These authors proposed that defect motion along grain boundaries, known to be responsible for electromigration failure in Al films, was also responsible for the observed $1/f$ noise. Black *et al.*[27] measured symmetry properties of resistivity fluctuations in thin films and found them to be nonscalar in a number of metals. They interpreted these results in terms of rotations of symmetry-breaking defects. Garfunkel and Weissman[28] studied noise statistics in metal resistors of very small volume to estimate conduction-electron–scattering cross sections of the individual microscopic processes responsible for the noise. For most metals (except Nb) they found cross sections less than 10^{-15} cm^2, consistent with expected cross sections for point defects in metals. Several theoretical models have also been proposed to explain the noise magnitude in terms of defect motion.[29–32]

In this paper we report the results of a number of experiments performed to study the dependence of $1/f$ noise in Cu films on a particular class of defects: those created by high-energy electron and ion irradiation. The films described here were irradiated while cooled below room temperature inside a high-voltage transmission electron microscope (TEM), and the sample noise and resistance were measured *in situ*. Since the change in average resistance is proportional to the added defect concentration,[33] changes in the noise can be directly related to the number of added defects. In this way we address several questions concerning the identity, structure, and kinetics of the defects responsible for the radiation-induced $1/f$ noise. We initially used the Hitachi HU-650 TEM at the National Center for Electron Microscopy at Lawrence Berkeley Laboratory (LBL), and later the Kratos AEI-EM7 1200-keV TEM and Ion-Beam Interface at the High-Voltage Electron Microscope/Tandem Facility at Argonne National Laboratory (ANL). Parts of this work have been presented elsewhere.[21,34,35]

In this paper we refer to the extensive literature concerning radiation damage in metals, much of which is concerned with freely suspended bulk materials of high crystalline quality. The interpretation of this work involves a detailed knowledge of irradiation conditions and sample properties (e.g., dimensions, purity, initial defect structure, crystalline orientation, etc.) The complex nature of our own samples (thin films, small crystallites, probable oxidation at surfaces and grain boundaries, the presence of a substrate) makes quantitative comparison with previous work on bulk materials uncertain, though qualitative similarities are evident and will be used to interpret our results. We do, however, caution against attempts to overinterpret the data presented here in terms of detailed concepts of defect structures and dynamics established for bulk, crystalline Cu.

II. EXPERIMENTAL METHODS

For the LBL experiments we evaporated 99.99%-pure Cu in a (5×10^{-7})-Torr vacuum to produce 100-nm-thick polycrystalline Cu films on room-temperature $\langle 100 \rangle$ Si wafers with a 350-nm amorphous SiO_2 layer. Standard photolithography and wet chemical etching were used to produce a (90×4)-μm^2 central structure with five large contact pads [Fig. 1(a)]. The wafers were diced into 9-mm squares (one structure per square) and annealed at 400 °C for 1 h at a pressure below 10^{-5} Torr. TEM later revealed continuous films with occasional small pinholes and typical grain sizes of 100–200 nm. We used an acid etch to produce a small hole in the reverse side of the wafers, stopping the process before it penetrated the SiO_2 layer on the front side, thereby producing a SiO_2 "window" roughly 300 μm in diameter within 50 μm of each Cu central structure [see Fig. 1(a)]. This window (partially transparent to electrons) allowed us to position the beam of the TEM on the central structure.

For the ANL experiments we cut 3-mm disks from an oxidized Si wafer and etched each disk to produce a "window." We then used a liftoff process to pattern ~100-nm films, evaporated form 99.9999%-pure Cu, into the geometry shown in Fig. 1(b). In some samples the Cu was doped with small amounts of In or Be. We made

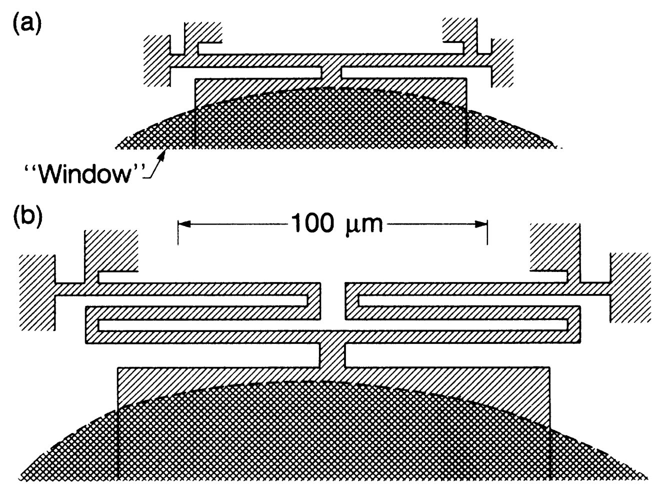

FIG. 1. Hatched regions are top-view configurations of samples used at (a) LBL and (b) ANL. A freely suspended SiO_2 "window" (cross-hatched) within 50 μm of each sample is used to position electron beam to cover the five-probe central structure.

most of these doped samples by electron-beam evaporation of dilute alloy sources in a vacuum of 2×10^{-8} Torr. All samples used at ANL were annealed as described above and stored in a dry N_2 desicator.

In the LBL experiments, prior to insertion of the sample the electron beam was aligned at low magnification ($\sim 500\times$) and the electron flux was measured via a Faraday cup located below the camera plane. Spatial and temporal nonuniformities in the electron-beam intensity introduced approximately a $\pm20\%$ relative uncertainty in the electron dose ϕ; the absolute dose calibration was uncertain by roughly a factor of 2. The electron dosimetry of the TEM at ANL has been described in detail elsewhere.[36] During each irradiation the electron flux was monitored continuously to an accuracy of several percent by a Faraday cup positioned next to the sample image in the TEM viewing chamber. For samples irradiated at 90 K, the part of the electron beam used for dosimetry passed through the freely suspended amorphous SiO_2 "window" before reaching the Faraday cup. The transmission efficiency of 1.1-MeV electrons through the window (typically around 50%) was measured at room temperature for each sample and used to determine the absolute electron dose. On samples Cu-01 and Cu-05 the sample "windows" were broken to allow an unobstructed electron path to the Faraday cup.

For the LBL experiments the samples were mounted on a single-tilt liquid-nitrogen (LN_2) cold stage which could operate over a temperature range 90–300 K. A small LN_2 reservoir outside the TEM cooled a Cu rod extending to the TEM optical axis, where the sample, a wire-wound heater, and a platinum-resistance thermometer (PRT) were mounted. The thermal time constant of the system was roughly 5 min, which ensured sufficient temperature stability for accurate noise measurements. Thin Cu wires were attached to the five contact pads by pressed In disks. For the ANL experiments the samples were mounted on a single-tilt liquid-He-flow cold stage[36] designed to achieve low base temperatures (~ 8 K) and rapid temperature cycling over a range 8–200 K. A system with feedback to a He exhaust valve could maintain the average temperature to better than 0.1 K over a temperature range 8–300 K. However, the thermal time constant of the sample block became quite small at low temperatures. Small fluctuations in sample temperature made low-level sample-noise measurements unreliable below 70 K, and introduced some extra system noise (with roughly a $1/f^2$ spectrum) for $70<T<150$ K.

For the LBL experiments we used a four-terminal multimeter to obtain the resistance to better than 0.1%; to determine resistivity, one multiplies the resistance by the geometry factor $G_F\equiv wd_e/l$, where w and l are the sample width and length, and d_e is the "electrical" sample thickness. Uncertainties in the measured sample dimensions produced a 30% error in the absolute resistivity, which was about $10^{-6}\Omega$ cm at 90 K, compared with 3×10^{-6} Ω cm at room temperature. The automated apparatus[36] at ANL could measure the resistance in samples cooled below 10 K to better than 0.01%. In order to be consistent with previous work by King and coworkers,[37] all measurements at ANL were analyzed using an "effective" geometry factor

$$G_F^*\equiv\frac{\rho_b(H)-\rho_b(L)}{R_H-R_L}\;, \tag{3}$$

where $\rho_b(T)$ is the known bulk resistivity of pure Cu at a temperature T, and R_H and R_L are the measured resistances at an elevated temperature H ($\simeq 300$ K) and low temperature L ($\simeq 8$ K), respectively. Any systematic effects which produce a difference between G_F^* and the true G_F (e.g., a softened phonon spectrum in the films relative to the bulk Cu) are expected to affect all the samples in roughly the same way. For all the ANL samples we take the sample dimensions to be the measured values of l and w, and use an "effective" sample thickness $d^*\equiv(l/w)G_F^*$, which may differ from the measured thickness d_m. These parameters are summarized in Table I. Typically, $d^*/d_m\simeq 0.88$ ($\pm10\%$); we take $\pm15\%$ as an estimate of the absolute uncertainty in d, G_F, and $\Delta\rho$.

The inset of Fig. 4 shows the five-terminal bridge circuit used to measure low-frequency resistance fluctuations, following a suggestion by Voss and Clarke.[38,39] A sample with five contacts and resistance $R_s\sim 10$ Ω formed two arms of a Wheatstone bridge, each arm with approximately equal resistance. Large, wire-wound resistors with resistances of ~ 1000 Ω were used in the other two arms, and the bridge was driven by a bias voltage $V_B(t)=V_0\cos(2\pi f_0 t)$, where $f_0\sim 2010$ Hz. A 50-Ω ten-turn potentiometer and a variable air capacitor were used to balance the bridge. The signal voltage across the bridge was amplified by a liquid-nitrogen-cooled transformer (Triad G-4 with a turns ratio of ~ 50) connected to a low-noise Brookdeal 5004 preamplifier, filtered through a (1–3)-kHz passband and demodulated with a lock-in detector. The output was filtered over a (0.1–25)-Hz passband and analyzed with a digital spectrum analyzer in conjunction with a desktop computer. This ac measurement scheme avoided preamplifier $1/f$ noise, allowed us to match the sample to the preamplifier optimally, and helped minimize effects of low-frequency pickup transients present inside the TEM. The transformer was cooled to reduce the Nyquist noise in the transformer windings[40] to a level lower than the Nyquist noise of the samples at 90 K. The contact noise was checked by measuring the noise with different bias resistors, and was found to be insignificant.

To analyze the excess low-frequency noise, we subtracted the background-noise spectral density without current modulation (predominantly the Nyquist noise of the sample) from the spectral density in the presence of the current. At least 50 scans were averaged for each spectral density. For the LBL measurements, least-squares linear fits were made to log-log plots of the data to obtain the noise magnitude and slope to better than $\pm5\%$. For the ANL measurements a routine which minimized the goodness-of-fit parameter χ^2 was used to fit the noise data to a function of the form

$$S_V(f)\simeq A/f^m+B/f^2\;, \tag{4}$$

where A, B, and m are free fitting parameters. The first term is the sample $1/f$ noise and the second is $1/f^2$ noise

TABLE I. Thin-Cu-film samples used at Argonne National Laboratory. RRR is the room-tempereerature–to–helium-temperature residual-resistance ratio. Sample width w is measured by an optical microscope; the physical thickness d_m is measured with a stylus profiler or a calibrated quartz-crystal monitor during deposition. All samples had nominal length $L=480$ μm. The effective geometry factor G_F^*, the effective thickness d^*, and the initial trapping term Q_0 are defined in the text.

Sample	RRR	G_F^* (nm)	w (μm)	d^* (nm)	d_m (nm)	d^*/d_m	Q_0 (nΩ cm)
Cu-01	5.72	0.732	4.6	87	100	0.87	
Cu-02	4.80	0.842	4.8	85	100	0.85	6.7
Cu-03	6.41	0.732	4.0	88	100	0.88	3.9
Cu-04	7.40	0.821	3.8	105	120	0.88	6.5
Cu-05	6.95	0.727	3.3	106	120	0.88	
Cu-06	7.40	0.803	3.8	103	120	0.86	4.8
CuIn-1[a]	5.89	1.081	4.7	112	140	0.80	14.0
CuIn-2[b]	4.40	0.883	4.2	95	104	0.91	38.0
CuBe-1[c]	5.73	0.978	3.4	139	145	0.96	7.3
CuBe-2[d]	5.93	0.857	4.0	104	120	0.87	10.6

[a]Pellet-drop thermal evaporation. Indium content, ~270 at. ppm, determined by x-ray-fluorescence spectroscopy.
[b]Electron-beam evaporation. Indium content, ~0.45 at. %, determined by Rutherford backscattering.
[c]Thermal evaporation. Source material had ~680 at. ppm Be. Low trapping efficiency thought to be due to oxidation of Be during thermal evaporation [A. Baily (private communication)]. Sample $1/f$ noise not measured.
[d]Electron-beam evaporation. Source material ~680 at. ppm Be.

introduced by small temperature fluctuations of the cold stage. These fits accurately yield the $1/f$ noise magnitude at higher frequencies (the B/f^2 term was always less than 10% of the A/f^m term for $f>5$ Hz). However, a rather large "trough" of roughly constant χ^2 often existed in the free-parameter space, which produced large uncertainties in the parameter m.

III. EXPERIMENTAL RESULTS

A. LBL results

Since vacancies and interstitials migrate freely and recombine at room temperature,[33] it was necessary to cool the samples to 90 K or lower during irradiation in order to build up a substantial excess defect population. Test irradiations performed at room temperature produced no measurable increase in sample noise or resistivity. After measuring the resistance and noise in a sample at 90 K, we irradiated the sample with a beam of 500-keV electrons with a typical intensity of 10^{17} cm^2 s^{-1} for a specified time. Using the sample resistance as a thermometer, we established that the sample temperature rose by at most 1 K during irradiation. After each irradiation, which sometimes lasted for more than 1 h, we measured the resistance and noise. Typically 30 min elapsed between the irradiation and the noise measurements. At the end of this sequence we annealed the film for 5 min at each of a series of progressively higher temperatures, remeasuring the resistance and noise at 90 K after each annealing step. The noise magnitude remained constant (within ±5%) for up to 2 h, provided the sample was maintained at 90 K. All the data taken at LBL reported here are from a single Cu sample. Similar results were observed in two other samples.

To understand the results to be presented, we first review some fundamentals concerning radiation damage in Cu. High-energy electrons, ions, or neutrons[33] can create defects in bulk crystalline Cu, via a collision-recoil process. When sufficient energy is transferred to a recoiling Cu atom in a sample held at a temperature $T<20$ K, a "replacement collision sequence"[41] [Fig. 2(a)] can lead to the creation of stable defects in the form of "Frenkel pairs" (vacancy-interstitial pairs).[33] The vacancy is simply a vacant lattice site (with some surrounding lattice relaxation) while the most stable interstitial complex is the so-called ⟨100⟩ "dumbbell" [Fig. 2(b)] where two atoms share a single site. The electrical resistivity ρ increases with Frenkel-pair concentration by $\Delta\rho \simeq \rho_F C$, where C is the fractional concentration of Frenkel pairs and[37] $\rho_F \simeq 2.75\times10^{-4}$ Ω cm. The minimum "threshold energy" $T_{d,\min} \sim 19$ eV necessary to create stable Frenkel

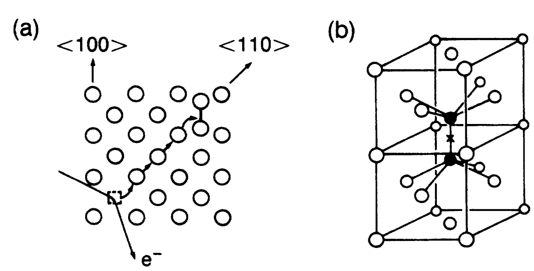

FIG. 2. Frenkel pairs in fcc metals: (a) replacement collision sequence leading to production of Frenkel pair (from Ref. 41) and (b) "dumbbell" ⟨100⟩ split interstitial in fcc metals.

pairs in Cu corresponds to a minimum incident-electron energy $E_{min} \simeq 390$ keV. In pure, bulk Cu one ideally expects the defect-production rate to be negligible for $E < E_{min}$, and to increase rapidly for $E > E_{min}$. In practice, small levels of "subthreshold" damage[42,43] are often observed for $E < E_{min}$. This damage is not fully understood, but is thought to be connected to the presence of light-atom impurities or initial defect structure (e.g., dislocations).

Incident electrons with kinetic energy in the 1-MeV range generate spatially uncorrelated Frenkel pairs uniformly in thin Cu samples. These defects are translationally immobile below 20 K, but can undergo thermally activated migration at higher temperatures, as evidenced by a number of "recovery stages" of the added resistivity observed in annealing experiments.[33] Recovery in the "stage-I" temperature range (0–60 K) is due to interstitial motion. Close-pair[33] recombination is observed when $20 < T < 40$ K, while for $40 < T < 60$ K the remaining interstitials migrate freely until they recombine with vacancies, cluster with other interstitials, or are trapped at suitable sites (impurity atoms, dislocations, grain boundaries, etc.). Recovery in the "stage-II" range (60–220 K) is thought to be related to the thermally activated release of interstitials from traps.[33] The most prominent feature in the stage-III range (220–330 K) is a strong recovery step attributed to the onset of free migration[44] of monovacancies.[45]

For irradiation at 90 K, the accumulation of immobile vacancies and migrating interstitials has been successfully described by the "unsaturable" trap"[46] model: an interstitial can recombine with its own vacancy ("correlated" recombination), migrate and recombine with another vacancy, or be trapped at an impurity atom, dislocation, etc. The free-interstitial concentration is sufficiently small that the chance of interstitial clustering is negligible. As the vacancy concentration increases, migrating interstitials are more likely to recombine with vacancies than be trapped, and the radiation damage rate $d\,\Delta\rho/d\phi$ should vary as

$$\frac{d\,\Delta\rho}{d\phi} \simeq g\rho_F(1+\Delta\rho/Q)^{-1} . \tag{5}$$

Here, ϕ is the electron dose (fluence), g is a generation term describing the production of freely migrating interstitials, and the trapping term

$$Q = \rho_F C_t(r_t/r_v) , \tag{6}$$

where C_t is the fractional trap concentration, and r_t and r_v are the trap and vacancy capture radii, respectively. If g and Q do not depend strongly on $\Delta\rho$, this expression can be integrated to yield the result that, for large ϕ, $\Delta\rho \sim \phi^{1/2}$. This scaling has been well documented in bulk materials.[33]

Figure 3 shows the change in sample resistivity $\Delta\rho$ versus the total 500-keV electron dose ϕ, for three irradiation sequences on the same sample at 90 K, each separated by a room-temperature annealing process of a least 12 h. We see that $\Delta\rho$ scales approximately as $\phi^{1/2}$, consistent with the behavior observed in bulk materials at

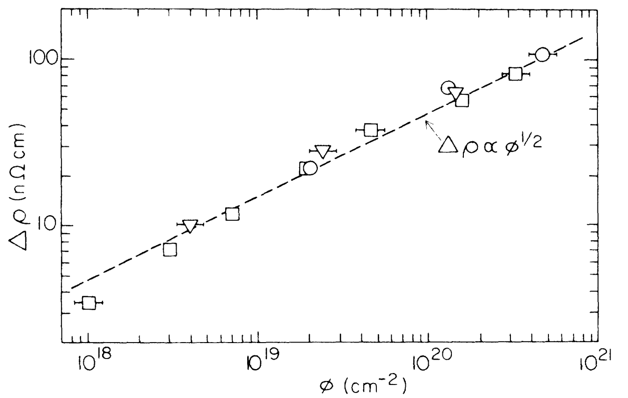

FIG. 3. Change in sample resistivity $\Delta\rho$ at 90 K vs 500-keV electron dose ϕ for three different irradiation sequences. The dashed line $\Delta\rho \propto \phi^{1/2}$ is drawn through the data by eye. Data taken at LBL.

similar temperatures, and described by the "unsaturable trap model."[46] The observed initial damage rate, $d\,\Delta\rho/d\phi$, is, however, significantly larger (approximately a factor of 5) than that observed in bulk materials under similar irradiation conditions.[47,48] Even though the absolute dose calibration could be in error by as much as a factor of 2, this damage rate still appears large compared with previous measurements. Tests performed on thicker (~300-nm) Cu films indicated a lower 500-keV damage rate, while a 100-nm film which had not been annealed at 400 °C following evaporation was found to have a damage rate more than a factor of 3 larger than well-annealed films of the same thickness. A significant amount of "subthreshold damage" for electron energies < 390 keV was also observed in these samples. These results will be discussed later in conjunction with the work at ANL.

Figure 4 shows several voltage power spectra $S_V(f)$ (with background noise subtracted) for the sample biased

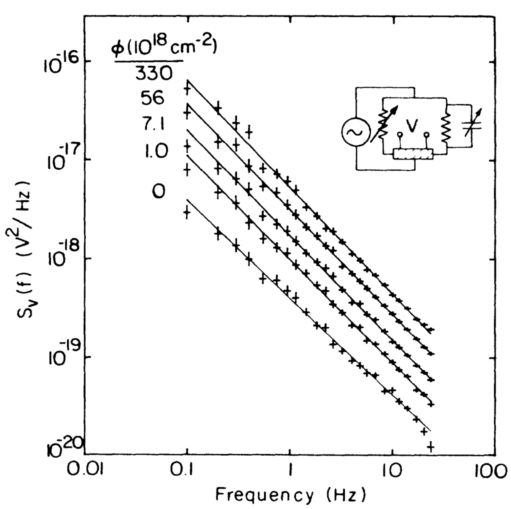

FIG. 4. Typical excess-voltage-noise power spectra and least-squares fits for different electron doses ϕ. The vertical error bars represent one standard deviation; the horizontal bars are not significant. Data taken at LBL. Inset: ac-bridge configuration.

with a current $i_{rms} \approx 20$ mA, but with progressively higher electron doses. The balance of the noise-measurement bridge was trimmed after each irradiation, though the required adjustment was always small. The spectral density of the $1/f$ noise increases by more than an order of magnitude as radiation-induced defects are added to the film, showing that defects are a source of $1/f$ noise in metal films. This large increase in noise magnitude is accompanied by only about a 10% increase in sample resistivity. In Fig. 4 the slope of the spectral density steepens by about 10%, most of the increase occurring after the first irradiation. The noise remains $(1/f)$-like over the full range of irradiations.

We now characterize the noise in terms of the parameters[49] m and α. In Eq. (1), V is twice the rms voltage across half the sample, $N \simeq 2.9 \times 10^{12}$ ($\pm 30\%$) is the estimated number of atoms in the sample, and $f_0 = 1$ Hz. Before each irradiation sequence the initial value of α at 90 K was within 10% of 5.5×10^{-4}. In Fig. 5 we plot $\Delta\alpha$ versus $\Delta\rho$ for the three data runs illustrated in Fig. 3; $\Delta\alpha$ and $\Delta\rho$ are the changes in α and ρ relative to the values before a particular run. The values of $\Delta\alpha$ obtained after successive irradiations fall approximately on the dashed line $\Delta\alpha \propto \Delta\rho^{0.6}$. Since $\Delta\rho$ is roughly proportional to the added fractional Frenkel-pair concentration C_d ($C_d \equiv C_v \simeq C_i$), these data indicate that the noise magnitude scales as $C_d^{0.6}$. At first sight, this dependence is surprising. If all the added defects act as equivalent, independent, local noise sources, one would expect α to scale linearly with C_d. However, we note that C_d is a measure of the *total* number of added defects, but it is not necessary that all the added defects contribute equally to the noise. For example, existing defect-noise models[25–28] relate the noise magnitude only to the concentration C_m of *mobile* defects which change position or orientation in the same frequency range as the observed noise. Since C_d is an upper limit on C_m, one can use these noise measurements to check whether a particular noise model is able to produce sufficient noise levels.[31,50] The observed scaling $\Delta\alpha \propto C_d^{0.6}$, however, may be primarily an indication of how C_m scales with C_d, rather than how the noise magnitude depends on C_m.

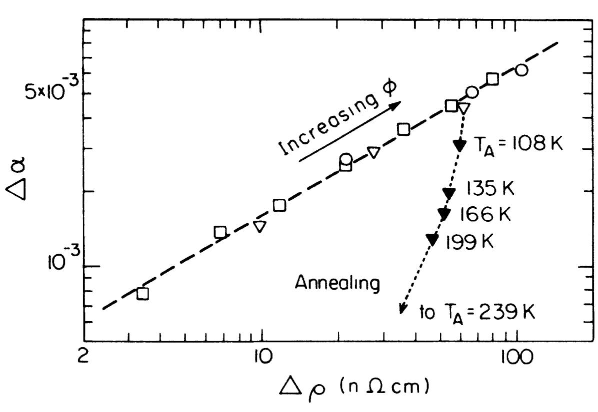

FIG. 5. Change in $(1/f)$-noise magnitude $\Delta\alpha$ vs change in sample resistivity $\Delta\rho$. Dashed line $\Delta\alpha \propto \Delta\rho^{0.6}$ is drawn as a guide to the eye. Points along this line correspond to increasing electron dose ϕ, while points along the dotted line correspond to annealing at successively higher temperatures. The point for $T_A = 239$ K (not shown) is $\Delta\rho \simeq 11.6$ nΩ cm, $\Delta\alpha \simeq 7 \times 10^{-5}$.

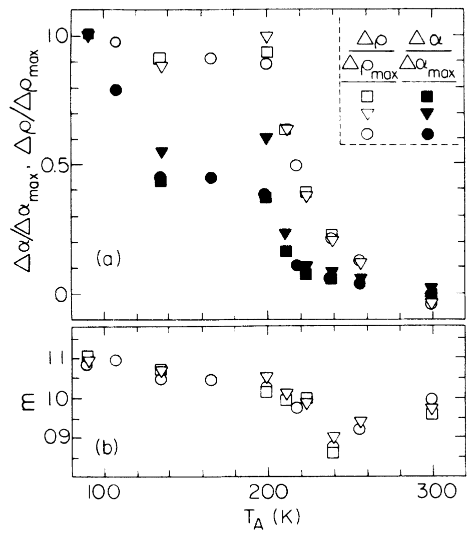

FIG. 6. Annealing behavior of an irradiated Cu film with $\Delta\rho_{max} \approx 90$ nΩ cm and $\Delta\alpha_{max} \approx 6 \times 10^{-3}$ prior to annealing. (a) Recovery of the $(1/f)$-noise magnitude ($\Delta\alpha/\Delta\alpha_{max}$) and resistivity ($\Delta\rho/\Delta\rho_{max}$) vs annealing temperature T_A. (b) Frequency exponent m vs annealing temperature T_A.

The dependence of $\Delta\alpha$ on $\Delta\rho$ after the samples were annealed is very different, as is shown by the dotted line in Fig. 5. The annealing process reduces the noise much more rapidly than the resistivity, producing hysteresis in the plot of $\Delta\alpha$ versus $\Delta\rho$. This behavior is also illustrated in Fig. 6(a), which shows the annealing data plotted as recovery curves, namely $\Delta\rho/\Delta\rho_{max}$ and $\Delta\alpha/\Delta\alpha_{max}$ versus the annealing temperature T_A. The three different symbols in the figure correspond to three separate measurement sequences, taken on different days. Most of the resistivity recovery occurs in the range $200 < T_A < 300$ K, and is similar to the "stage-III recovery" well documented for irradiated Cu.[33] This recovery step is generally associated with the onset of the free migration of monovacancies.[44] The noise magnitude, $\Delta\alpha$, recovers partially over this same temperature range, but also exhibits substantial recovery below 150 K that is not readily apparent in the resistivity curves. These data support the idea that certain subpopulations of the added defects (e.g., mobile defects) contribute disproportionately to the noise. The observed difference in the recovery of $\Delta\rho$ and $\Delta\alpha$ is readily explained if one assumes that a population of "noisy" defects is deactivated (via thermally activated trap release, recombination, or clustering, for example) at lower temperatures than most of the added defects.

This interpretation is consistent with a model ascribing the noise to defect motion, since thermally activated defect motion is also known to be responsible for defect annealing observed in irradiated metals.[33] The type of defect motion which leads to annealing may well be related to motions which produce noise. Such a relation between annealing and noise is quite plausible, but for the moment it is only hypothetical. We emphasize here that by "mobile" and "noisy" we refer only to defects which move at a given temperature with characteristic frequencies within our experimental bandwidth (0.1–25 Hz). In a broader sense, essentially all the added defects are actually mobile, since they are metastable and will migrate and recombine if one heats the samples and/or waits a sufficiently long time.

In addition to the changes seen in α and ρ, the exponent m measured at 90 K also changed during the irradiation and annealing experiments. Figure 4 shows that m increased from about 1.0 to 1.1 over the irradiation sequence. The annealing behavior of m in Fig. 6(b) exhibits a striking dip to a value $m \simeq 0.9$ at $T_A \approx 240$ K that is reproducible in all the samples studied at LBL. We see from the figure that this behavior is extremely repeatable on a single sample, provided it was annealed at room temperature for an extended period between runs. We note that this dip occurs within the range of annealing temperatures where the "stage-III" recovery of $\Delta\rho$ and $\Delta\alpha$ is observed; temperatures at which large changes in the added defect population occur. We will return to this behavior later.

All the noise measurements described so far were taken with the sample maintained at $\sim$90 K. Additional information about the noise-generation processes can be gained from the temperature dependence of the added noise. In particular, one can check whether the added noise is thermally activated in a manner consistent with a model proposed several years ago by Dutta, Dimon, and Horn.[18]

In the next series of measurements, a sample at 90 K was first irradiated with 500-keV electrons to a total resistivity increment $\Delta\rho \approx 85$ nΩ cm, and annealed at a temperature $T_A > 90$ K. The $1/f$ noise was measured as a function of temperature for $T < T_A$. By first annealing at T_A, one puts the sample into a state such that any remaining noise measured at $T < T_A$ is quasistationary, i.e., the noise magnitude and spectral shape do not change significantly during the noise measurement.

In Fig. 7(a) the noise magnitude is plotted as a function of T, for $T_A = 201$ K, $T_A = 239$ K, and in the unirradiated (i.e., fully annealed) state. We use the parameter ρ_*^2 instead of α since electron-phonon scattering causes ρ to change substantially as the temperature is increased. We see from Fig. 7(a) that the noise magnitude is a very strong function of the sample temperature T and the sample state (as determined by T_A). The noise level on a single sample can be made to vary by well over 2 orders of magnitude by varying T and T_A. The three curves in Fig. 7(a) are quadratic fits to the three sets of data points. In Fig. 7(b) the frequency exponent m is plotted as a function of T for the same data series shown in Fig. 7(a). The parameter m also has a strong dependence on both T and T_A. The curves shown in Fig. 7(b) are discussed below.

If the $1/f$ noise arises from an ensemble of thermally activated processes with a distribution in activation rates, its spectral density should, in general, be described by a superposition of thermally activated Lorentzians.[19,20] Du Pre[19] and subsequently Dutta *et al.*[18] considered such a

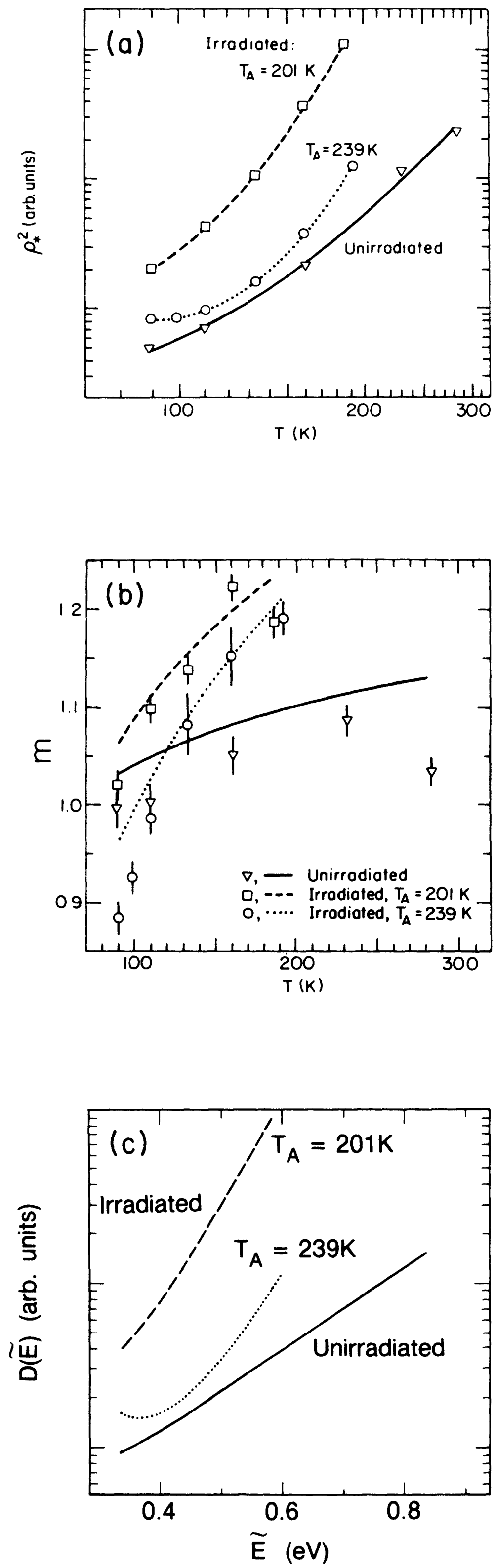

FIG. 7. Temperature dependence of induced $1/f$ noise. (a) Noise magnitude ρ_*^2 vs T for Cu film in unirradiated state, and for $\Delta\rho_{max} \approx 85$ nΩ cm followed by a 5-min anneal at T_A. Curves are log-log quadratic fits to the data points. (b) m vs T for data series in (a). Curves are prediction of Eq. (9) using fits in (a). (c) Distribution of noise activation energies in film. Curves are calculated using fits in (a) and Eqs. (7) and (8)

model in which (1) the distribution of activation rates results primarily from a distribution $D(E)$ in activation energies E, and (2) the coupling of the process to the measured noisy quantity (e.g., sample resistance) is temperature independent. With these assumptions, these authors showed that $1/f^m$ noise (with $m \simeq 1$) follows provided $D(E)$ is much broader than $k_B T$ (k_B is Boltzmann's constant), but otherwise of arbitrary form. According to this model, the shape of $D(E)$ can be determined from the measured quantity $S_\rho(f,T)$, via the relation

$$D(\tilde{E}) \sim (f/T) S_\rho(f,T) \; . \tag{7}$$

Here,

$$\tilde{E} \equiv -k_B T \ln(2\pi f \tau_0) \; , \tag{8}$$

where τ_0^{-1} is the attempt rate of the activated process, assumed constant for all E. Dutta *et al.*[18] extended the analysis to show that the temperature dependencies of $S_\rho(f,T)$ and m in such a model are related by

$$m(f,T) = 1 - \frac{1}{\ln(2\pi f \tau_0)} \left[\frac{\partial \ln S_\rho}{\partial \ln T} - 1 \right] . \tag{9}$$

The noise measured in a physical system is not consistent with this model unless it obeys this relation.[51]

The curves shown in Fig. 7(b) are the temperature dependencies of m for the three annealing states predicted from Eq. (9) and the fits of the data in Fig. 7(a), assuming $\tau_0^{-1} \sim 10^{14}$ s^{-1}, a typical phonon frequency. The curves reproduce the general trends in the measured data points rather well, indicating that the noise observed with the sample in all three annealing states is thermally activated in a manner consistent with the model of Dutta *et al.*[18]

Weissmann[52] and Scofield *et al.*[53] have pointed out that qualitative agreement of Eq. (9) with experiment is not a sufficient condition to prove that the observed noise results from a process with a broad spread of activation energies. An alternate model,[52,53] with a single activation energy and an appropriate distribution in the attempt rate τ_0^{-1}, could also result in noise of the form $1/f^m$, and would obey a consistency relation which is qualitatively very similar to Eq. (9). One expects that $1/f$ noise, which has been observed to agree qualitatively with Eq. (9), could, in general, result from a distribution in E and in τ_0. In certain small metal-oxide-semiconductor field-effect transistor[6-8] (MOSFET) and tunnel-junction devices[9-11,13] the low-frequency excess noise can be decomposed into a discrete set of Lorentzians, with τ_0 and E determined for each Lorentzian. In these systems substantial distributions in both τ_0 and E are in fact found.

With this said, one should not forget that one of the most attractive features of the model of Dutta *et al.*[18] is that a $1/f^m$ spectrum follows in a natural way from a broad (but otherwise arbitrary) distribution $D(E)$. On the other hand, a model which assumes a fixed E_0 and a distribution $H(\tau_0)$ in τ_0 requires that $H(\tau_0) \sim \tau_0^{(m-2)}$ to produce $1/f^m$ noise. In this case one must provide the physical motivation for such a distribution in τ_0. We note that a number of studies indicate the existence of a variety of defect motions in metals with typical activation energies in the range[33] 0.1–3 eV and with attempt rates[41,54,55] within a few orders of magnitude of 10^{12} s^{-1}. The model of Dutta *et al.*, which assumes that the range in rates is dominated by a range in activation energy, is probably the most appropriate for our results.

With this assumption, we use the data in Fig. 7(a) with Eqs. (7) and (8) to infer the form of $D(E)$, shown in Fig. 7(c), over an energy range determined by the measurement temperatures. For $T_A \simeq 200$ and 240 K we see a pronounced increase in $D(E)$ as E nears 0.6 eV. This energy is close to measured activation energies for the migration of monovacancies,[33] suggesting that there is a relation between the activation energies of those defect motions which cause noise and those which lead to migration. This same general conclusion can, of course, be drawn directly from Figs. 6 and 7(a) by noting that the irradiated films become extremely noisy close to 200 K, a temperature at which defect migration causes a large-scale reduction in the defect concentration.[33]

We see from Fig. 7(c) that, at a given value of E, $D(E)$ decreases monotonically with T_A, as one might expect if noisy defects are removed during annealing. The shape of $D(E)$ does, however, change in a subtle way. For $T_A \simeq 240$ K, $D(E)$ has a local minimum near $E \sim 0.4$ eV, which is not present for $T_A \simeq 200$ K, nor when the film is fully annealed. Since $D(E)$ and $m(f,T)$ are linked via Eqs. (7) and (9), this behavior implies that the value of m measured at ≈ 100 K should, as a function of T_A, start off larger than 1 for $T_A < 200$ K, drop below 1 for $T_A \approx 240$ K, then increase for larger T_A. This is precisely the "dip" observed in Fig. 6(b). In this analysis the dip observed in m (measured at 90 K) that occurs near $T_A \approx 240$ K is a consequence of the evolution of the *shape* of $D(E)$ as the sample is annealed. At this point we can offer no physical insight into the reason why the local minimum in $D(E)$ near $E \sim 0.4$ eV should appear at $T_A \approx 240$ K. We can only note that in samples held at 240 K vacancy migration has commenced, and large-scale reduction and redistribution of defects occur.

Finally, we note qualitative similarities between the results presented in Fig. 7 and those described by Fleetwood and Giordano.[23] These authors measured noise changes due to thermal annealing of defects present in AuPd films freshly sputtered onto room-temperature substrates. As in our study, Fleetwood and Giordano found that the noise magnitude increased strongly with temperature, especially near temperatures where annealing caused large changes in sample noise and resistivity. They also found that changes in $S_\rho(f,T)$ caused by annealing were systematically reflected in the behavior of $m(T)$, consistent with Eq. (9). Thus, even though the types of defects and their activation energies for annealing were quite different from those in ours, the overall behavior of the noise during defect annealing was quite similar.

B. ANL results

Several experiments at ANL were performed at low temperatures, where the damage-rate studies are much more indicative of the fundamental defect-production processes. Analysis of damage rates at elevated temperatures is complicated by defect migration. The solid squares in Fig. 8(a) show the measured low-temperature damage rate $d\,\Delta\rho/d\phi$ versus $\Delta\rho$ for sample Cu-01 irradiated with 1.1-MeV electrons. The geometry of this sample is similar to that shown in Fig. 1(b), except in that the SiO_2 window was broken to allow an unobstructed path for electron-dose calibration. The dashed line in Fig. 8(a) is the expected bulk damage rate, which for Cu is a linear function intersecting the vertical axis[48,56] at $\sim 6\times 10^{-27}$ $\Omega\,cm^3$, and the horizontal axis[48,57] at $\Delta\rho \simeq \rho_\infty \simeq 750$ nΩ cm. The linear decrease in the bulk damage rate with increasing added defect concentration results from the spontaneous recombination of interstitials (vacancies) created close to existing vacancies (interstitials), and from subthreshold annealing effects.[57] The measured damage rate is fairly close to the bulk rate and appears to decrease linearly at high $\Delta\rho$, but also exhibits enhanced damage below $\Delta\rho \sim 20$ nΩ cm, which introduces some curvature into the plot. This curvature appears, at first glance, qualitatively similar to that measured in several other radiation-damage experiments on thin films.[36,48,58] In those studies this effect is thought to result from the deviation of the measured resistivity ρ from the intrinsic bulk resistivity ρ_b due to Fuchs-Sondheimer[59,60] size corrections for boundary scattering.

In order to test whether such corrections are important in our experiments, we applied the Fuchs-Sondheimer theory to the data in Fig. 8(a) using extrapolation formulas and numerical tables calculated by Groeger.[61] To apply this theory one requires the sample thickness d and two materials-dependent parameters: the fraction P of electrons scattered specularly at the surfaces (the remainder are assumed to scatter diffusely) and the constant $\kappa = \rho_b l_b$, where l_b is bulk mean free path. The open diamonds and circles in Fig. 8(a) are the adjusted data with P chosen to be 0.4 and 0.0, respectively, assuming $\kappa \simeq 6\times 10^{-12}$ $\Omega\,cm^2$. Depending on the value of P, the magnitude of the damage rate can be modified substantially by such corrections. However, the curvature in the data seen at low $\Delta\rho$ cannot be eliminated for any reasonable choice of κ and P, and thus does not result simply from a Fuchs-Sondheimer effect.

The adjusted damage-rate curves were each fitted with a phenomenological expression

$$\frac{d\,\Delta\rho}{d\phi} = A\,(1-\Delta\rho/B) + C\exp(-\Delta\rho/D)\ . \tag{10}$$

The first term represents the expected bulk damage rate, which decreases linearly with $\Delta\rho$. The second term approximates the "anomalous" damage observed at small $\Delta\rho$. In order to determine an appropriate value of the parameter P, we varied P to obtain the known bulk value for $B \simeq \rho_\infty \simeq 750$ nΩ cm. This was achieved with the reasonable values $\kappa \simeq 6\times 10^{-12}$ $\Omega\,cm^2$ and $P \simeq 0.4$, and is shown by the open diamonds in Fig. 8(a). The solid line is the fit of Eq. (10) to the adjusted data. The adjusted initial damage rate $A \simeq 5.2\times 10^{-27}$ $\Omega\,cm^3$ is within experimental uncertainties of the bulk value 6×10^{-27} $\Omega\,cm^3$. The other adjusted parameter values are $C \simeq 0.8\times 10^{-27}$ $\Omega\,cm^3$ and $D \simeq 14$ nΩ cm. The "anomalous" part $C\exp(\Delta\rho/D)$ represents only a small fraction of the total damage rate. We thus conclude that most of the radiation-induced defects in these films are similar to those expected in bulk Cu.

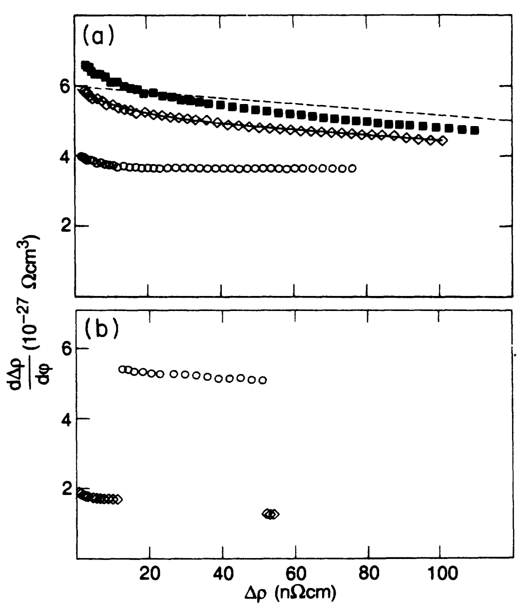

FIG. 8. Low-temperature damage rate $d\,\Delta\rho/d\phi$ vs $\Delta\rho$. (a) Sample Cu-01; solid squares are measured 1.1-MeV electron damage rate and dashed line is expected bulk Cu damage rate. Open symbols are size-effect–corrected data (see text), with $\kappa = 6\times 10^{-12}$ $\Omega\,cm^2$, and $P = 0.4$ (open diamonds) or 0.0 (open circles). Solid curve is fit of Eq. (10) to open-diamond data points. (b) Damage rate in sample Cu-05, due to 500-keV (diamonds) or 1.1-MeV (circles) electron irradiation.

In Fig. 8(b) we plot the low-temperature damage rate due to electron irradiation of different energies for sample Cu-05, in which the SiO_2 window was broken to allow an unobstructed electron path. The damage rate due to 1.1-MeV electrons (open circles) is very similar in form and magnitude to the bulk rate and to that measured in sample Cu-01. The 500-keV damage rate (open diamonds) is lower than the 1.1-MeV rate, but is nevertheless a factor of 2–3 larger than the expected bulk value[37,56] for polycrystalline Cu.

We noted earlier that the LBL experiments indicated that thicker films had lower 500-keV damage rates than thinner ones, and that annealing the films (at 400 °C) prior to irradiation significantly reduced the damage rate. Both observations are consistent with the proposal that small grain size is responsible for the enhancement. King and co-workers[62] have done preliminary studies on freely suspended Cu films grown on substrates at liquid-nitrogen temperatures as a succession of thin ($\sim$ 10-nm) layers so that the crystal structure was extremly small. The initial 500-keV He-temperature damage rate in these films was found to be over an order of magnitude larger than the bulk Cu value, and exhibited substantial subthreshold damage. It has been tentatively suggested that this anomalous damage might result from "interrupted"[62] replacement collision sequence [see Fig. 2(a)], due to the presence of fine-grained structure.

Most thin-film Cu samples used by King and coworkers[36,37,48] had much larger grain size and exhibited bulk damage rates for 500-keV to 1.1-MeV electron irradiation.[37,48] These films were thicker (typically 200–400 nm) than the samples used here, were deposited in clean conditions on substrates held at room temperature or above, and were irradiated while freely suspended. We are not certain why the films in the current study, which were deposited in a similar manner, appear to show enhanced damage rates at 500 keV. We suspect that the presence of a substrate may affect the film grain structure. The Si substrate and the Cu film also have significantly different thermal expansion coefficients, which result in a very large internal strain ($\sim 0.15\%$) in the Cu as it is cooled from room temperature to low temperatures.

These low-temperature measurements indicate that the 1.1-MeV damage rate in the Cu films is close to the bulk rate, suggesting that most of the defects created by 1.1-MeV electrons are bulklike vacancy-interstitial pairs. The defect population resulting from 1.1-MeV electron irradiation at 90 K is then expected to be primarily in the form of trapped interstitials and isolated, nonmigrating vacancies. These defects are possible sources of the induced $1/f$ noise.

To investigate whether trapped interstitials, in particular, are primarily responsible for the radiation-induced noise, we measured the noise at 90 K in nominally "pure" (undoped) Cu films and in Cu films intentionally doped with In and Be. In bulk Cu these impurities are known to act as interstitial traps. An isolated indium atom is an oversized impurity which traps interstitials with a moderate trapping energy[54,63] of about ~ 0.3 eV. Interstitials trapped at isolated In impurities are mostly released at temperatures below 150 K. Furthermore, internal-friction measurements[54,55] indicate that interstitials trapped at In impurities can undergo low-frequency, thermally activated rotations around the In atoms in the temperature range 30–150 K. Such trapped interstitials are prime suspects for the source of low-frequency noise. Beryllium, on the other hand, is an undersized impurity with a much stronger trapping energy.[54,63] Ultrasonic attenuation measurements indicate that interstitials trapped at Be impurities undergo a very rapid "hopping" motion around the Be atom, with MHz hopping rates at liquid-helium temperatures.[64] One therefore does not expect such defects to contribute to low-frequency noise. No *a priori* statements can be made concerning the expected noise behavior of residual traps present in all the films.

To estimate the effective trap concentrations in the films, we made measurements of the "reciprocal damage rate" $d\phi/d\,\Delta\rho$ at 90 K, due to 1.1-MeV electron irradiation. Referring to Eq. (5), we see that $d\phi/d\,\Delta\rho$ should be linear in $\Delta\rho$, provided g and Q are independent of $\Delta\rho$ (i.e., the defect concentration). In fact, g and Q do depend weakly on $\Delta\rho$.[63,65]. For the purposes of this paper, we use the initial slope of a plot of $d\phi/d\,\Delta\rho$ versus $\Delta\rho$ to estimate the initial trapping term Q_0 and we use Eq. (6) to estimate the trap concentrations in the different Cu films.

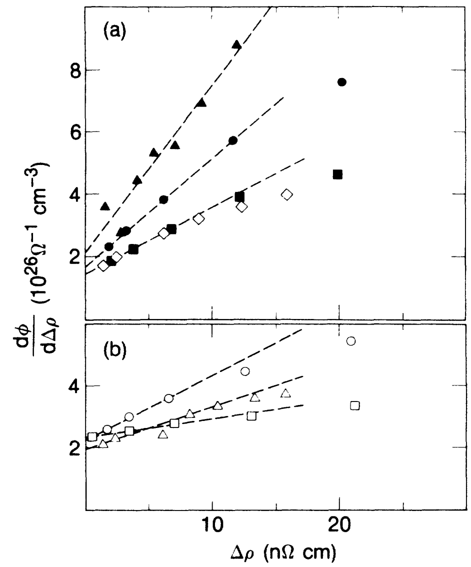

FIG. 9. 90-K reciprocal damage rate $d\phi/d\,\Delta\rho$ vs $\Delta\rho$ measured on seven samples following 1.1-MeV electron irradiation. (a) Undoped samples: Cu-0.3 (solid triangles), Cu-06 (solid circles), Cu-04 (solid squares), and Cu-02 (open diamonds). (b) Doped samples: CuBe-2 (open circles), CuIn-1 (open triangles), and CuIn-2 (open squares). Dashed lines are linear fits to initial data points (see text). Sample properties summarized in Table I.

In Fig. 9 we plot $d\phi/d\Delta\rho$ versus $\Delta\rho$ for several of the films listed in Table I. After each irradiation the sample was allowed to remain at 90 K for 10 min before being cooled to about 8 K for the resistivity measurement. The intercept with the vertical axis on such a plot gives the intrinsic defect-production rate, which should be roughly independent of trap concentration, while the initial slope is related to the trap concentration. Figure 9 shows that the initial value of $d\phi/d\,\Delta\rho$ is roughly the same for all samples, but that there is a large range of initial slopes. We estimated these initial slopes by linear fits for $\Delta\rho \lesssim 10$ nΩ cm, shown by dashed lines. The corresponding values of Q_0 are listed in Table I. If one assumes that the interstitial trapping radius r_t and the vacancy capture radius r_v are approximately equal for all traps observed here, these values of Q_0 indicate trap concentrations which range from about 15–25 at. ppm for the undoped films, and 40–50 at. ppm for the CuBe and lightly doped CuIn films, to 140 at. ppm for heavily doped CuIn. In the indium-doped films, these trap concentrations are significantly less than the measured impurity concentrations. In these films many traps may consist of clustered rather than isolated In atoms. The main point is that there does exist a large range of trap concentrations in the films.

In Fig. 10 we plot the change in the noise magnitude $\Delta(\rho_*^2)$ measured at 80 K as a function of $\Delta\rho$ for six different samples, doped and undoped, following irradiation at 90 K. We see that $\Delta(\rho_*^2)$ increases with $\Delta\rho$ by nearly the same amount in all cases, even though the films had different types of traps, and a factor-of-10 varia-

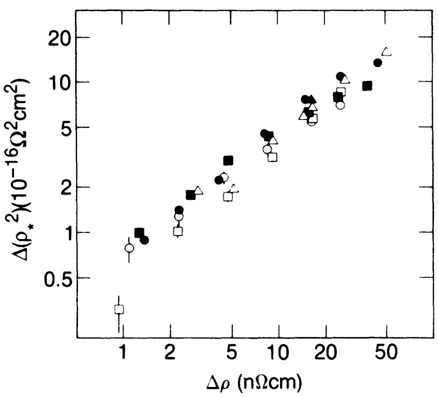

FIG. 10. Change in (1/f)-noise magnitude $\Delta(\rho_*^2)$ measured at 80 K vs $\Delta\rho$ for six Cu films following 1.1-MeV electron irradiation at 90 K. Solid symbols are undoped Cu; open symbols are doped Cu. Symbols defined in Fig. 9. Noise reference frequency $f_0 = 5$ Hz [see Eq. (2)].

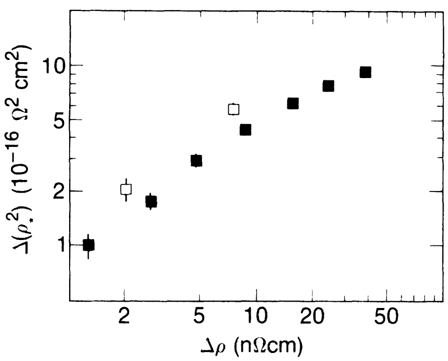

FIG. 11. Change in noise magnitude $\Delta(\rho_*^2)$ at 80 K vs $\Delta\rho$ for sample Cu-06 following 500-keV electron irradiation (open squares) or 1.1-MeV electron irradiation (solid squares) at 90 K. Reference frequency $f_0 = 5$ Hz.

tion in effective trap concentration. It is convenient to define the "specific noise" γ_ρ,

$$\gamma_\rho \equiv \frac{\partial(\rho_*^2)}{\partial(\Delta\rho)} , \tag{11}$$

representing the induced noise per added defect. In Fig. 10 a single line can be drawn which falls within $\sim 30\%$ of all but the most uncertain (lower left) data point, indicating that the specific noise γ_ρ is quite insensitive to the type and quantity of interstitial traps present in the film.

If one assumes that trapped interstitials are responsible for the induced noise, then one must produce a microscopic mechanism for the noise (e.g., an interstitial rotation, rearrangement, etc.) which is not sensitive to the type and average occupancy of the traps. This might prove difficult, as there are known differences in trapping strength between different impurities,[54,63] leading one to expect differences in any noise-producing motions. If, on the other hand, one assumes that vacancies are responsible for the noise, then the "specific noise" should be independent of trap type and concentration. We will return to this possibility later.

All the data in Fig. 10 were taken from samples irradiated with 1.1-MeV electrons. One can also compare, on a single sample, the noise induced by defects created with electron irradiation of different energies. In Fig. 11 we show $\Delta(\rho_*^2)$ versus $\Delta\rho$ for sample Cu-06 after 500-keV and 1.1-MeV electron irradiation. We see that the specific noise is $\sim 40\%$ higher for the 500-keV irradiation than for the 1.1-MeV irradiation, indicating that an "average" defect created by 500-keV electrons is somewhat noisier than that created by 1.1-MeV electrons. These results will be discussed later.

Due to their relatively larger mass, ions can deliver much more energy to a recoiling lattice atom than an electron with equivalent kinetic energy. The median recoil energy $T_{1/2}$ (the energy below which one-half of the defects are created) of the lattice Cu atom varies[66] from roughly 40 eV for 1-MeV electrons, to ~ 1 keV for 1-MeV protons, and ~ 50 keV for 1-MeV Kr. When $T_{1/2}$ is large, multiple defects are produced in spatially localized "displacement cascades."[66] The size of a cascade, in general, increases with increasing $T_{1/2}$, but eventually saturates for $T_{1/2} \gtrsim 30$ keV, as multiple subcascades are formed. When $T_{1/2} \gtrsim 30$ keV, computer simulations of the cascade dynamics indicate that roughly $\frac{2}{3}$ of the created Frenkel defects (which are stable at low $T_{1/2}$) spontaneously recombine immediately following cascade formation.[66] Many of the defects which do not spontaneously recombine collapse into clusters. At elevated temperatures many of the remaining defects undergo thermally activated *correlated* reactions within the cascade, but a fraction escapes clustering and recombination within the cascade and migrates freely through the lattice. Measurements of radiation-induced segregation in ion-irradiated metal alloys at 650–900 K have been used to estimate the relative efficiency for producing freely migrating defects[66] as a function of $T_{1/2}$. Such measurements on a Cu–1-at. % Au alloy indicate that, relative to the value for $T_{1/2} \sim 700$ eV, the efficiency for producing freely migrating defects drops from 100% to around 5% as $T_{1/2}$ is increased from about 700 eV to 50 keV. Measurements on other fcc metal systems (including pure Cu) with other techniques and different irradiation temperatures agree with these efficiencies[66] to within a factor of 3. These efficiencies are normalized to the *total* defect production. If they are instead normalized relative only to defects which *survive* spontaneous postcascade recombination, the relative efficiency drops from 100% to the order of 15% with increasing $T_{1/2}$. Thus, for these higher recoil energies most of the surviving defects are in the form of large clusters, and only a small fraction are able to migrate and react as isolated interstitials and vacancies. One intuitively expects that the "specific noise" resulting from such a defect configuration will be quite different from that due to electron irradiations.

Figure 12 compares the 1/f noise in sample Cu-02 following 1.1-MeV electron and 1-MeV Kr^+ irradiation at 90 K. The electron irradiations preceded the ion irradiations, and the two measurements were separated by an extended room-temperature annealing process. The specific noise γ_ρ is significantly larger for defects created

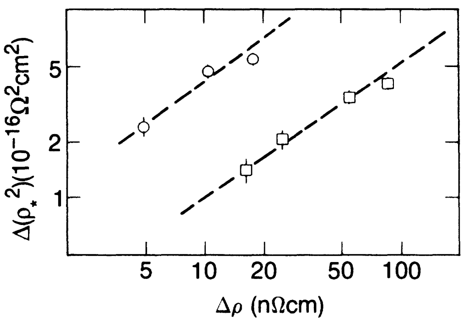

FIG. 12. Change in noise magnitude $\Delta(\rho_*^2)$ at 80 K vs $\Delta\rho$ for sample Cu-02 following 1.1-MeV electron irradiation (open circles) or 1-MeV Kr^+ irradiation (open squares) at 90 K. Dashed lines are guides to the eye. Reference frequency $f_0=5$ Hz.

by electron irradiation than for those created by Kr^+ ions. One requires roughly a factor of 8 times the value of $\Delta\rho$ for the Kr^+ irradiations to achieve the same noise level found in the film following electron irradiation. Similar results were also obtained from sample CuIn-01. When compared with the estimated fractions of isolated and clustered defects in the ion-irradiated films, these data suggest that isolated defects are primarily responsible for the added $1/f$ noise, and that most (if not all) the added noise observed following Kr^+ irradiation is due to the fraction of the defects which remain isolated.

IV. DISCUSSION

Our experimental results give direct evidence that radiation-induced defects are a source of $1/f$ noise in Cu films. However, we are also interested in the mechanism by which a defect motion produces a resistance fluctuation. Several authors have recently pointed out that quantum-mechanical interference of electrons scattered from lattice defects should produce resistance fluctuations as the defects move.[27,29–32,52] Electron-defect–scattering calculations of Martin[67,68] have been used to quantify "local-interference" effects,[31] which were then applied to the radiation-induced $1/f$ noise discussed here. It was found that local reorientations and/or rearrangements of anisotropic defects (e.g., ⟨100⟩ interstitials, divacancies, etc.) could plausibly account for the magnitude of this radiation-induced $1/f$ noise, provided a sufficient fraction of the added defects reorient.

Since a variety of defect configurations can, in general, result from electron and ion irradiation, we wish to identify the particular defect types responsible for the induced noise. In this section we consider several models, each of which assumes that a particular type of defect is primarily responsible for the induced noise. We compare each model with our experimental results and with the "local-interference" model.[31]

Model A. We first consider a model in which one assumes that the noise does not result from crystalline defects within the film at all, but rather from some interaction of the resistivity with defects created in the underlying substrate. This model is not consistent with a number of experimental results. The damage-rate measurements discussed earlier indicate that the added resistivity is primarily due to defects within the Cu. From Fig. 6(a) we see that there exists a direct correlation between the recoveries of the induced noise and the added resistivity in the annealing temperature range 200–300 K, temperatures at which migration of monovacancies occurs in bulk Cu.[33] These observations indicate a correlation between the induced noise and defects within the Cu film.

Model A is also inconsistent with the results shown in Fig. 10. If the induced noise results only from defects within the substrate, then it should depend only on ϕ and not on the trap concentration within the film. Undoped Cu films at 90 K must be irradiated to a larger values of ϕ than doped films to build up a given value of $\Delta\rho$, since there are fewer impurities present to trap interstitials. One would therefore expect a plot of $\Delta(\rho_*^2)$ versus $\Delta\rho$ to behave roughly as sketched in Fig. 13(a), with the undoped films becoming increasingly noisier as $\Delta\rho$ increases. This expected behavior is not consistent with the experimental results shown in Fig. 10.

One can also consider the possibility that the induced noise results simply from the small amount of vacancy-interstitial recombination which occurs during the noise measurements. Such recombination causes the sample resistivity to decrease monotonically in time as Frenkel pairs randomly recombine. It can be shown[69] that such "recombination noise" can account for neither the magnitude nor the spectral shape of the induced noise.

We now consider several models which attribute the induced noise primarily to trapped interstitials. Before considering specific cases, we make the general point that an isolated ⟨100⟩ interstitial and an interstitial-impurity complex are both anisotropic defect structures which, in accordance with the discussion in Ref. 31, should produce substantial resistivity fluctuations if the defects reorient.

Model B. One assumes that interstitials trapped at dopant atoms are significantly noisier that those at residual traps and that they are the dominant noise source in the Cu films. By "residual" we mean traps which are present in all the films in roughly equal concentrations. From such a model one would expect that the doped

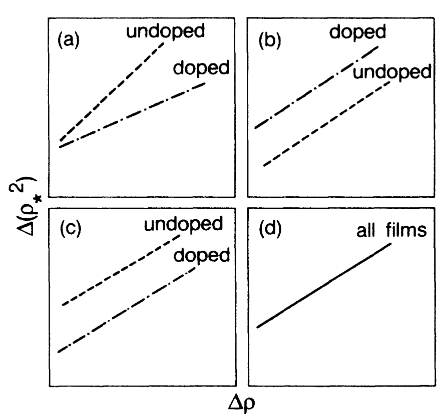

FIG. 13. Behavior of $\Delta(\rho_*^2)$ vs $\Delta\rho$ predicted by various models (see text). (a) Model A, (b) model B, (c) model C, and (d) models D–F.

films would have significantly larger specific noise than the doped films, for all values of $\Delta\rho$. This expected behavior is sketched in Fig. 13(b). It is not consistent with the measured behavior shown in Fig. 10, which shows the specific noise to be roughly independent of trap concentration.

Model C. Interstitials at residual traps are assumed noisier than those at dopant atoms, and are assumed to be the dominant noise source. Since only a fraction of the trapped interstitials in the doped films are at residual sites, one would expect the undoped films to be noisier, as sketched in Fig. 13(c). This result is inconsistent with the data..

Model D. All trapped interstitials produce approximately equal noise levels, independent of trap type and occupancy. This behavior, sketched in Fig. 13(d), is consistent with the behavior shown in Fig. 10, and cannot be ruled out. However, it is not physically intuitive that interstitials trapped at different impurities should exhibit similar noise behavior. This is especially true if one compares oversized impurities (e.g., In) with undersized impurities (Be), which are known to have quite different trapping energies and interstitial-impurity defect structures.[54,63] Here we must qualify our experimental conclusions somewhat since the active-trap concentration in our Be-doped samples is only a factor of 2 larger than in the undoped films. Further experiments with higher Be trap concentrations are desirable to determine whether or not there might yet exist subtle differences between the noise behavior of the undoped films and those doped with undersized and oversized impurity traps.

Before considering other possible noise sources, we note that any model which attributes the bulk of the noise to trapped interstitials is not consistent with the measurements summarized in Fig. 7(a), which shows that the irradiated films become extremely noisy when heated near 200 K. Near this temprature, vacancies are known to migrate in bulk Cu, whereas the trapped interstitials merely recombine with the migrating vacancies.

Model E. Isolated vacancies within the bulk produce the noise. In this case the added noise should be independent of trap type, concentration, and average occupancy, consistent with the results in Fig. 10. One might also expect intuitively that the noise should increase as the irradiated films are heated close to temperatures at which vacancies migrate, as shown in Fig. 7(a). On a physical basis, however, it is hard to understand how any kind of motion of a bulklike, symmetric, isolated vacancy could produce a resistance fluctuation.[31] A rotation of a monovacancy has no physical significance, and a simple translation from one lattice site to another simply reproduces the local environment around the vacancy.

Model F. Vacancies close to a surface, grain boundary, dislocation, or some other extended defect structure are assumed primarily responsible for the noise. A translation of such a vacancy changes the local environment of the defect and produces a resistivity fluctuation. By "close" we mean a distance no greater than a Fermi wavelength $\lambda_F \sim 0.5$ nm, in accordance with the "local" interference effects discussed in Ref. 31.

Figure 11 offers additional information: The specific noise γ_ρ resulting from 500-keV electron irradiation is larger than that from 1.1-MeV electrons. This is somewhat counterintuitive, since the structure and distribution of stable defects in bulk Cu resulting from electron irradiation is not significantly different at these two energies. One difference is, however, that any subthreshold effects[43] are expected to be fractionally more important at the lower energy, since the intrinsic (bulk) damage rate is roughly an order of magnitude smaller at 500 keV then at 1.1 MeV. Earlier we suggested that the anomalously high damage rates measured for 500-keV electron irradiation were due to a subthreshold damage mechanism related to small-scale crystallite structure within the films. If, in fact, a subthreshold mechanism enhances defect production near surfaces and grain boundaries, model F would predict that γ_ρ should be larger for 500-keV irradiation than for 1.1 MeV. Further experiments involving a range of film thickness and grain size and a wider range of electron energies would help determine whether there is a relation between the film structure and the enhanced damage production and the enhanced γ_ρ observed at lower electron energies.

Model F is consistent with the experimental results, and with the requirement that a defect change its local environment when it moves. However, one expects only those vacancies located close to a surface, grain boundary, etc., which we refer to as *boundary* vacancies, will be available to contribute to the noise. One can estimate the fraction F of the vacancies close to a boundary by the expression $F \sim 6\lambda_F/D$, where D is the dimension of a typical crystallite, assumed roughly cubical. For $\lambda_F \sim 0.5$ nm and $D \sim 100$ nm, one finds $F \sim 0.03$. In Ref. 31, estimates were made of the fraction of the total number of added defects which must move at frequencies within the experimental bandwidth in order for local-interference effects to account for the induced noise. These fractions were of the order 0.05–0.5. If expressed relative only to boundary vacancies, these required fractions must be larger by a factor of F^{-1}. Consequently, one must require nearly all the boundary vacancies to be mobile in order that local-interference effects account for the induced $1/f$ noise.

However, one should not rule out model F simply on this basis, since several parameters in the local-interference model and the above analysis are rather uncertain. For example, the noise magnitude predicted by Eq. (8) of Ref. 31 scales as β^2, where β is the anisotropy parameter of a defect. A value of $\beta \sim 0.15$ was assumed. The actual value of β could conceivably differ from this number by as much as a factor of 3, with a corresponding change in the predicted noise level of up to an order of magnitude. Also, the fraction F defined above is a very rough estimate. The actual fraction F of "boundary vacancies" could be considerably larger in the films contained large numbers of dislocations or other extended defects within the Cu grains. Finally, we note that model F is similar to a proposal made by Koch *et al.*[26] that the $1/f$ noise measured in evaporated Al films was due to the motion of vacancies along grain boundaries.

To summarize, models A–C are all inconsistent with the experimental results. Models D and E are both consistent with Fig. 10, but each has problems. Model D would require that all trapped interstitials produce roughly equal noise levels, and the model does not offer an obvious reason why the noise should increase dramatically at temperatures where vacancies migrate. With model E it is not clear how the motion of a symmetric monovacancy can result in a resistance fluctuation. Model F appears to be most consistent with experimental results and theoretical requirements of local-interference effects but has some trouble account for the magnitude of the induced noise.

Finally, it should be noted that none of these models has considered the effects on the damage rate or induced noise of the very large internal strain ($\sim 0.15\%$) present in the Cu films. Further experiments in which the films are subject to variable internal stress may prove useful in determining whether internal stress is connected to the radiation-induced noise.

V. SUMMARY AND CONCLUSIONS

We have used high-energy electron and ion irradiation of polycrystalline Cu films to study the relationship between $1/f$ noise and defects in metals. The radiation-induced $1/f$ noise increases in a systematic way with the number of defects introduced, indicating a direct connection between $1/f$ noise and defects in metals. The difference in the recovery of the induced noise and the added resistivity after successive annealing steps suggests that a large fraction of the induced noise is generated by a subpopulation of "noisy" defects, presumed to be mobile, that are more readily annealed than the majority of the added defects. The temperature dependences of the noise magnitude and the frequency exponent m after irradiation and partial annealing are consistent with the Dutta-Dimon-Horn[18] model, indicating that thermally activated kinetics govern the induced $1/f$ noise.

The low-temperature damage rates measured in the Cu films due to 1.1-MeV electron irradiation are found to be close to bulk Cu damage rates. In contrast, the 500-keV damage rates are found to be significantly higher than the correspondingly bulk damage rates. It is suggested that a subthreshold effect related to grain size within the films may be responsible for the enhanced 500-keV damage.

The measured reciprocal damage rates due to 1.1-MeV electron irradiations performed at 90 K were used to estimate the effective interstitial trap concentrations in undoped Cu films and films doped with In and Be. It was found that the specific noise γ_ρ, which is proportional to the induced noise per added defect, is not sensitive to the type and quantity of interstitial traps present in the films. Isolated defects introduced by electron irradiation appear to generate much more noise than the mainly clustered defects introduced by 1-MeV Kr^+ irradiation.

Several simple modes were examined to identify the defects responsible for the radiation-induced $1/f$ noise. A model which attributes the noise to the motion of vacancy-type defects close to surfaces, grain boundaries, or dislocations is most consistent with the experimental results and theoretical considerations.

In the future one could investigate the effects of the crystal grain structure on the induced noise, either by systematically varying the metal film thickness (to vary the average grain size), or by using epitaxially grown single-crystal films. A promising alternative to high-energy electrons would be high-energy proton irradiation. The 1-MeV proton damage rate in Cu is sufficiently large[33] that only a modestly focused (~ 1 mm) beam in a typical accelerator would be necessary to obtain a reasonable damage rate, yet the average primary recoil energy from these protons is sufficiently small (~ 1 keV) that most of the defects produced would be in the form of isolated Frenkel pairs.[66] One could also investigate the effect on the induced noise of internal stress in the metal films. This could be achieved either by using various substrate materials with different coefficients of thermal expansion, or by applying external stress to a cold sample. Finally, other metals besides Cu should be studied; for example, aluminum. Small interstitial clusters in aluminum are known to reorient in the temperature range 20–60 K, producing peaks in the low-frequency internal friction observable at several temperatures.[41,54] Such interstitial reorientations could also show up as peaks in the low-frequency noise.

Note added. We note that Ralls and Burhman[70] have recently observed two-level resistance fluctuations in a Cu nanostructures, with activation energies, attempt frequencies, and scattering–cross-section changes suggestive of defects moving between metastable configurations. These results are consistent with our observations of noise activation energies and scattering–cross-section changes[31] of radiation-induced defects in Cu films.

ACKNOWLEDGMENTS

We thank R. Hammond and P. Rosenthal for assistance with the electron-beam evaporations, D. Jurica for assistance at the National Center for Electron Microscopy at LBL, and E. A. Ryan and S. Ockers for assistance at the High-Voltage Electron Microscopy/Tandem Facility at ANL. We are grateful to R. Giauque, L. E. Rehn, and J. Baker for sample analysis, and K. Haga and A. C. Baily for assistance with equipment at ANL. We thank R. Benedek, E. E. Haller, R. Gronsky, L. E. Rehn, C. W. Allen, K. L. Merkle, H. Wiedersich, R. C. Birtcher, and R. S. Averback for valuable advice and assistance. One of us (J.P.) acknowledges receipt of financial assistance from the IBM Corporation, and from the Argonne Division of Educational Programs, funded by the U.S. Department of Energy. This work was supported by the Director, Office of Energy Research, Office of Basic Energy Sciences, Materials Sciences Division of the U.S. Department of Energy under Contracts No. DE-AC03-76SF00098 and No. W-31-109-ENG-38.

*Present address: IBM Research Division, Thomas J. Watson Research Center, P.O. Box 218, Yorktown Heights, NY 10598.

†Present address: Chemistry and Materials Science Department, Lawrence Livermore National Laboratory, Livermore, CA 94550.

[1]P. Dutta and P. M. Horn, Rev. Mod. Phys. **53**, 497 (1981).

[2]M. B. Weissman, Rev. Mod. Phys. **60**, 537 (1988).

[3]M. B. Weissman, R. D. Black, P. J. Restle, and T. Ray, Phys. Rev. B **27**, 1428 (1983).

[4]S. Lifson, G. Gavish, and S. Reich, Biophys. Struct. Mech. **4**, 53 (1978).

[5]S. Bhattacharya, J. P. Stokes, Mark. O. Robbins, and R. A. Klemm, Phys. Rev. Lett. **54**, 2453 (1985).

[6]K. S. Ralls, W. J. Skoçpol, L. D. Jackel, R. E. Howard, L. A. Fetter, R. W. Epworth, and D. M. Tennant, Phys. Rev. Lett. **52**, 228 (1984).

[7]M. J. Uren, D. J. Day, and M. J. Kirton, Appl. Phys. Lett. **47**, 1195 (1985).

[8]M. J. Kirton and M. J. Uren, Appl. Phys. Lett. **48**, 1270 (1986).

[9]C. T. Rogers and R. A. Buhrman, Phys. Rev. Lett. **53**, 1272 (1984).

[10]C. T. Rogers and R. A. Buhrman, Phys. Rev. Lett. **55**, 859 (1985).

[11]K. R. Farmer, C. T. Rogers, and R. A. Buhrman, Phys. Rev. Lett. **58**, 2255 (1987).

[12]Roger H. Koch, John Clarke, W. M. Goubau, J. M. Martinis, C. M. Pegrum, and D. J. Van Harlingen, J. Low Temp. Phys. **51**, 207 (1983).

[13]Bonaventura Savo, Frederick C. Wellstood, and John Clarke, Appl. Phys. Lett. **50**, 1757 (1987).

[14]Richard F. Voss and John Clarke, Phys. Rev. Lett. **36**, 42 (1976).

[15]H. G. E. Beck and W. P. Spruit, J. Appl. Phys. **49**, 3384 (1978).

[16]F. N. Hooge, Phys. Lett. **29A**, 139 (1969).

[17]John H. Scofield, Joseph V. Mantese, and Watt W. Webb, Phys. Rev. B **32**, 736 (1985).

[18]P. Dutta, P. Dimon, and P. M. Horn, Phys. Rev. Lett. **43**, 646 (1979).

[19]F. K. Du Pre, Phys. Rev. **78**, 615 (1950).

[20]A. Van der Ziel, Physica **16**, 359 (1950).

[21]Jonathan P. Pelz and John Clarke, Phys. Rev. Lett. **55**, 738 (1985).

[22]J. W. Eberhard and P. M. Horn, Phys. Rev. B **18**, 6681 (1978).

[23]D. M. Fleetwood and N. Giordano, Phys. Rev. B **31**, 1157 (1985).

[24]G. P. Zhigal'sky, Yu. Ye. Sokov, and N. G. Tomson, Radiotekh. Elektron. **24**, 410 (1979) [Radio Eng. Electron Phys. (USSR) **24**, 137 (1979)].

[25]D. M. Fleetwood and N. Giordano, Phys. Rev. B **28**, 3625 (1983).

[26]R. H. Koch, J. R. Loyd, and J. Cronin, Phys. Rev. Lett. **55**, 2487 (1985).

[27]R. D. Black, P. J. Restle, and M. B. Weissman, Phys. Rev. Lett. **51**, 1476 (1983).

[28]G. A. Garfunkel and M. B. Weissman, Bull. Am. Phys. Soc. **32**, 480 (1987).

[29]Sh. M. Kogan and K. E. Nagaev, Fiz. Tverd. Tela (Leningrad) **24**, 3381 (1982) [Sov. Phys.—Solid State **24**, 1921 (1982)].

[30]Shechao Feng, Patrick A. Lee, and A. Douglas Stone, Phys. Rev. Lett. **56**, 1960 (1986); **56**, 2772(E) (1986).

[31]Jonathan Pelz and John Clarke, Phys. Rev. B **36**, 4479 (1987).

[32]S. Herschfield, Bull. Am. Phys. Soc. **32**, 481 (1987).

[33]J. W. Corbett, *Electron Radiation Damage in Semiconductors and Metals* (Academic, New York, 1966).

[34]Jonathan Pelz and John Clarke, in *Noise in Physical Systems and 1/f Noise*, edited by A. D'Amico and P. Mazzetti (North-Holland, Amsterdam, 1986), p. 415.

[35]Jonathan Pelz, John Clarke, and Wayne E. King, in *Noise in Physical Systems*, edited by C. M. Van Vliet (World Scientific, Singapore, 1987), p. 507.

[36]Wayne E. King, Ph.D. thesis, Northwestern University, 1980.

[37]K. L. Merkle, Wayne E. King, A. C. Baily, K. Haga, and M. Meshi, J. Nucl. Mater. **117**, 4 (1983); Wayne E. King, K. L. Merkle, and Meshi, *ibid.* **117**, 12 (1983).

[38]Richard F. Voss and John Clarke, Phys. Rev. B **13**, 556 (1976).

[39]John H. Scofield and has independently developed similar appartus, Ph.D. thesis, Cornell University, 1985.

[40]D. E. Prober, Rev. Sci. Instrum. **45**, 849 (1974).

[41]W. Schilling, J. Nucl. Mater. **69&70**, 465 (1978).

[42]W. Bauer and A. Sosin, J. Appl. Phys. **35**, 703 (1964).

[43]J. Lauzier, P. Girard, and C. Minier, in *Internal Friction and Ultrasonic Attenuation in Solids*, edited by C. C. Smith (Pergamon, New York, 1979), p. 193.

[44]Th. Wichert, in *Point Defects and Defect Interactions in Metals*, edited by J. Takamuru, M. Doyama, and M. Kiritani (North-Holland, Amsterdam, 1982), p. 19; C. Minier and M. Minier, *ibid.*, p. 27.

[45]The bulk of the current experimental evidence supports this description, known as the "one-interstitial" model, which we use to interpret our results. A parallel interpretation using the alternate "two-interstitial" model (Refs. 33 and 50) is certainly possible. However, in contrast to Ref. 50, we do not believe that any results described here can be used to distinguish one model from the other and will make no statements as to their relative merits.

[46]R. M. Walker, in *Radiation Damage in Solids*, edited by D. S. Billington (Academic, New York, 1962), p. 594.

[47]A. Sosin and K. Garr, Phys. Status Solidi **8**, 481 (1965).

[48]Alan C. Baily, Ph.D. dissertation, Northwestern University, 1986.

[49]In comparing relative noise levels measured at 90 K, it makes little difference here whether one normalizes the noise using Eq. (1) or (2) since the sample resistivity changes by less than 10% as defects are added.

[50]A. Seeger, H. Stoll, and W. Frank, in Proceedings of the International Conference on Vacancies and Interstitials in Metals and Alloys, Berlin, 1986, edited by C. Abromeit and H. Wollenberger [Mater. Sci. Forum. **15-18**, 237 (1987)].

[51]Equation (9) is strictly obeyed only if the total variance of the noise is temperature independent (see Refs. 2 and 53); otherwise, there is a temperature-dependent offset in the two sides of Eq. (9). One typically expects this offset to be fairly small $[\sim 1/\ln(2\pi f \tau_0) \sim 0.03]$ and to vary slowly with temperature, allowing one to detect common *structure* on both sides of Eq. (9).

[52]M. B. Weissman, in *Proceedings of the Sixth International Conference on Noise in Physical Systems*, edited by P. H. E. Meijer, R. H. Mountain, and R. J. Soulen, U. S. Dept. of Commerce, Natl. Bur. Stand. (U.S.) Spec. Pub. No. 619 (U.S. GPO, Washington, D.C., 1981), p. 133.

[53]John H. Scofield, Joseph, V. Mantese, and Watt. W. Webb, Phys. Rev. B **34**, 723 (1986).

[54]K.-H. Robrock, in *Phase Transformations During Irradiation*, edited by F. V. Nolfi, Jr. (Applied Science, London, 1983), p. 115.

[55]G. Kollers, H. Jacques, L. E. Rehn, and K.-H. Robrock, J.

Phys. (Paris) Suppl. No. 10, **42**, 729 (1981).
[56]P. Jung, R. L. Chaplin, H. H. Fenzl, K. Reichelt, and P. Wombacher, Phys. Rev. B **8**, 553 (1973).
[57]G. Deusing, W. Sassin, W. Schilling, and H. Hemmerich, Cryst. Lattice Defects **1**, 55 (1969).
[58]Wayne E. King, K. L. Merkle, and M. Meshii, Phys. Rev. B **23**, 6319 (1981).
[59]K. Fuchs, Proc. Camb. Philos. Soc. **34**, 100 (1938).
[60]E. H. Sondheimer, Adv. Phys. **1**, 1 (1952).
[61]V. Groger, Cryogenics **19**, 56 (1979).
[62]Wayne E. King (unpublished).
[63]H. Wollenberg, J. Nucl. Mater. **69&70**, 362 (1978).
[64]L. W. Rehn, H. Wiedersich, and A. V. Granato, J. Phys. (Paris) Colloq. **46**, C10-67 (1985).
[65]R. Lennartz, F. Dworschak, and H. Wollenberg, J. Phys. F **7**, 2011 (1977).
[66]L. E. Rehn and P. R. Okamoto, in Proceedings of the International Conference on Vacancies and Interstitials in Metals and Alloys, Berlin, 1986, edited by C. Abromeit and H. Wollenberger [Mater. Sci. Forum. **15-18**, 985 (1987)].
[67]J. W. Martin, Philos. Mag. **24**, 555 (1971).
[68]J. W. Martin, J. Phys. F **2**, 842 (1972).
[69]Jonathan P. Pelz, Ph.D. dissertation, University of California–Berkeley, 1988.
[70]K. S. Ralls and R. A. Buhrman, Phys. Rev. Lett. **60**, 2434 (1988).